Research Article

Mercury Removal From Aqueous Solutions With Chitosan-Coated Magnetite Nanoparticles Optimized Using the Box-Behnken Design

Nadereh Rahbar [1,2,*]; Alireza Jahangiri [1,2]; Shahin Boumi [2]; Mohammad Javad Khodayar [3]

[1]Nanotechnology Research Center, Jundishapur University of Medical Sciences, Ahvaz, IR Iran
[2]Department of Medicinal Chemistry, School of Pharmacy, Jundishapur University of Medical Sciences, Ahvaz, IR Iran
[3]Department of Pharmacology and Toxicology, Toxicology Research Center, School of Pharmacy, Ahvaz Jundishapur University of Medical Sciences, Ahvaz, IR Iran

Corresponding author: Nadereh Rahbar, Department of Medicinal Chemistry, School of Pharmacy, Ahvaz Jundishapur University of Medical Sciences, Ahvaz, IR Iran. Tel: +98-6113738378, Fax: +98-6113738381, E-mail: n_rahbar2010@ajums.ac.ir

Background: Nowadays, removal of heavy metals from the environment is an important problem due to their toxicity.

Objectives: In this study, a modified method was used to synthesize chitosan-coated magnetite nanoparticles (CCMN) to be used as a low cost and nontoxic adsorbent. CCMN was then employed to remove Hg^{2+} from water solutions.

Materials and Methods: To remove the highest percentage of mercury ions, the Box-Behnken model of response surface methodology (RSM) was applied to simultaneously optimize all parameters affecting the adsorption process. Studied parameters of the process were pH (5-8), initial metal concentration (2-8 mg/L), and the amount of damped adsorbent (0.25-0.75 g). A second-order mathematical model was developed using regression analysis of experimental data obtained from 15 batch runs.

Results: The optimal conditions predicted by the model were pH = 5, initial concentration of mercury ions = 6.2 mg/L, and the amount of damped adsorbent = 0.67 g. Confirmatory testing was performed and the maximum percentage of Hg^{2+} removed was found to be 99.91%. Kinetic studies of the adsorption process specified the efficiency of the pseudo second-order kinetic model. The adsorption isotherm was well-fitted to both the Langmuir and Freundlich models.

Conclusions: CCMN as an excellent adsorbent could remove the mercury ions from water solutions at low and moderate concentrations, which is the usual amount found in environment.

Keywords: Chitosan; Magnetite Nanoparticles; Mercury

1. Background

Water, air, and soil pollution by heavy metals often originate from industry and are serious environmental problems. There is much current focus on methods of removal from natural waters and industrial waste waters to produce high quality water or to enable water recycling. Mercury is a heavy metal of primary concern because of its toxicity, persistence in the environment, and bioaccumulation. Techniques for mercury removal include traditional precipitation and coagulation methods, ion-exchange, solvent extraction, ultra filtration, and adsorption. The latter has attracted attention because of its effectiveness and ease of handling the adsorbent (1-4). Adsorbents used for mercury removal include activated carbon (5), modified chitosan (6-8), modified silica (2, 4), modified resin (9), and modified clay (10). Nanotechnology offers new and efficient ways for removal of organic and inorganic pollutants, especially in water, because of the high surface/volume ratio of nanomaterials (11-13). Among these, iron-based nanomaterials as solid phase extractors were promising in the removal of pollutants, because they are easily removed from a water solution using an external magnetic field (3, 14, 15).

Chitosan and its derivatives are effective and low-cost sorbents of heavy metals (16). Chitosan is a natural and harmless polysaccharide prepared by de-acetylating chitin widely used in food and pharmaceutical preparations and medical processes. It is capable of adsorbing a number of metals via its amino groups serving as ion-exchanges, or chelating sites, and can be easily modified by chemical and physical processes (17-23). Nanoparticles that incorporate the positive aspects of chitosan and magnetite nanoparticles (MNs) can be an effective sorbent for heavy metal removal from aqueous solutions, because there is an effective avenue to isolate nanomaterials after use (24-29).

Response surface methodology (RSM) with a Box-Behnken design (BBD) is a common statistical tool for optimization of variables affecting the removal process because

---

Implication for health policy/practice/research/medical education:
Mercury pollution in environment originates from industrial activities and is associated with several kinds of health problems in humans and amphibian. Due to such problems, mercury is in the list of chemical pollutants which needs to be more heavily monitored and removed due to its toxicity, persistence, accumulation in the environment and its effects on the nature health.

of relatively small number of systematic tests required, which reduces time, cost and resources. This experimental design can assess interaction effects between factors affecting adsorption and improve the removal of analyte (30-36).

2. Objectives

This study developed a procedure to remove mercury ions from an aqueous solution. RSM-BBD was used to optimize the operating factors for maximum mercury removal using these nanoparticles.

3. Materials and Methods

3.1. Reagents and Solutions

Chemicals of analytical grade and double distilled water were used in this study. A stock solution of Hg^{2+} (1000 mg/L) was purchased from Merck (Darmstadt, Germany). Diluted mercury solutions were prepared using successive dilutions of the stock solution. $FeCl_2.4H_2O$, $FeCl_3.6H_2O$, ammonia solution (25%), glacial acetic acid, sodium dodecyl sulfonate, dithizone, hydrochloric acid, and sodium hydroxide were purchased from Merck (Darmstadt, Germany). Chitosan (600-1200 cp and 96% degree of deacetylation) was purchased from Primex (Iceland).

3.2. Preparation of Chitosan-coated Magnetite Nanoparticles

The method of preparing CCMNs was developed by modifying published procedures (37, 38). Chitosan solution (1% w/v) was prepared by dissolving 0.1 g of chitosan flakes in 0.5 mL glacial acetic acid and diluting it with 10 mL distilled water. A 5 mL mixture of ferrous and ferric chlorides with a molar ratio of 1:2 was prepared and 50 mL of 1 M ammonium hydroxide solution was added drop-by-drop while stirring vigorously. Meanwhile, the chitosan solution was slowly dripped into the mixture. The mixture was stirred for 10 minutes, the prepared nanoparticles were collected using an external magnetic field and thoroughly washed with distilled water to remove excess ammonium hydroxide.

3.3. Characterization Methods

The Fourier transform infrared spectroscopy (FT-IR) spectra of the MNs and CCMNs were recorded using a Perkin-Elmer spectrometer (model BX2, USA), in the scanning range of 400-4000/cm. Scanning electron microscopy (SEM) was used to show the dimensions and morphology of the nanoparticles (TESCAN, model VEGA (II) LMH, Czech Republic). Energy dispersive x-ray diffraction (EDX) patterns of the nanoparticles were obtained at room temperature on a CTS cursor (Czech Republic).

3.4. Mercury Removal

The uptake procedure was performed in batch mode. The adsorption experiments were performed by mixing appropriate amounts of damp nanoparticles with 50 mL of mercury solution at a given concentration. Adjustment of the solution initial pH to the desired value was performed using HCl 0.1 mol/L and NaOH 0.1 mol/L solutions. After stirring for 10 minutes at room temperature at 150 rpm, the solid phase was removed from the solution using an external magnetic field. All experiments were performed in triplicate and the results were indicated as averages. The percentage of Hg^{2+} removed was calculated as:

1) $Removal, \% = 100 \times (C_0 - C_e)/C_0$

Where C_0 and C_e are the initial and equilibrium concentrations of Hg^{2+} in a solution of mg/L, respectively. The metal-loading capacity of the CMN at equilibrium was determined as:

2) $q_e, mg/g = (C_0 - C_e) \times V/W$

Where V is the volume of solution (L), and W is the amount of adsorbent (g).

3.5. Analytical Measurements

The concentration of mercury in solution after removal was analyzed using a UV-Vis spectrophotometer (Jasco 7800, Japan). Mercury-dithizone complex formed in an acidic solution with a maximum absorbance of 490 nm. Mercury determination was performed according to the standard methods slightly modified to achieve more sensitivity (39, 40).

3.6. Experimental Design

A three-level, three-factor Box-Behnken experimental design was employed to verify the performance of pH (5-8), the initial concentration of Hg^{2+} (2-8 mg/L), and the amount of damp adsorbent (0.25-0.75 g) in mercury removal and to determine optimum levels of these parameters. The Experimental range and level of independent variables are shown in Table 1. The percentage of Hg^{2+} removed was taken as the response of the system. Minitab 15 software was used to design the experiments. Table 2 shows the experimental design derived from BBD and the results of all 15 experiments, including three center points. Each experiment was performed in triplicate to verify reproducibility. The results were used to calculate the 10 coefficients of the second-order polynomial equation. This equation shows the relation between the desired response and the independent variables (pH, initial mercury concentration, and amount of adsorbent). Considering all linear, square, and linear-by-linear interaction terms, the second-order polynomial equation can be described as:

3) $Y = b_0 + b_1x_1 + b_2x_2 + b_3x_3 + b_{12}x_1x_2 + b_{13}x_1x_3 + b_{23}x_2x_3 + b_{11}x_1^2 + b_{22}x_2^2 + b_{33}x_3^2$

where Y is the response (percentage of Hg^{2+} adsorbed);

b0 is the offset term; b_1, b2, and b_3 are the linear coefficients; b_{11}, b_{22}, and b_{33} are the quadratic coefficients, and b_{12}, b_{13} and b_{23} are the coefficients of the linear-by-linear interaction effect between independent variables x_1 (pH), x_2 (initial concentration of Hg^{2+} solution), and x_3 (amount of adsorbent) (41). The goodness of fit of the model was assessed using a coefficient of regression (R^2) and analysis of variance (ANOVA).

4. Results

4.1. FT-IR and SEM Analysis for Adsorbent

Figure 1 shows the FT-IR spectra for (a) magnetite nanoparticles and (b) CCMN. The major bands in Figure 1A at 3392 and 598/cm are caused by the O-H stretching vibrations of the adsorbed water on the magnetite nanoparticles and the characteristic peak of Fe_3O_4, respectively. Figure 1B shows the adsorption band at 3406/cm caused by N-H and O-H stretching vibrations. The peaks at 1627 and 1403/cm correspond to the N-H bending vibration and C-N stretching vibration, respectively (25, 26, 37). The SEM micrographs for the magnetite nanoparticles and CCMNs are shown in Figure 2. As shown in Figure 2A, Fe_3O_4 particles have a spherical shape with a diameter distribution of 30-100 nm. Figure 2B indicates that the CCMN sizes are slightly larger than those of the magnetite particles. This observation is a result of chitosan coating the magnetite nanoparticles. The size of the particles remained in the nanometer range after coating, thus achieving the goal of preparing chitosan-coated nanoparticles.

4.2. Box-Behnken Statistical Analysis

ANOVA and α level of 0.05 (95% confidence) were used to determine the statistical significance of the independent variables and their interactions. The second-order polynomial coefficients and statistical parameters were analyzed using Minitab 15 software to describe the results. ANOVA for the quadratic model for mercury adsorption onto the CCMNs is shown in Table 3. The regression model F value of 46.63 and α value < 0.001 are highly significant. ANOVA showed that all effects were statistically significant (P < 0.05) at 95% confidence levels, except for the first order main effect of the initial concentration of mercury ions (P = 0.889), the second-order pH (P = 0.124),

Table 1. Experimental Range and Level of Independent Variables

Factors Range and Levels (Coded)	-1	0	1
Hg^{+2} concentration, mg/L	2	5	8
pH	5	6.5	8
Wet absorbent amount, g	0.25	0.50	0.75

Table 2. Box-Behnken Design Matrix for Three Variables-three Levels Together With Observed and Predicted Values

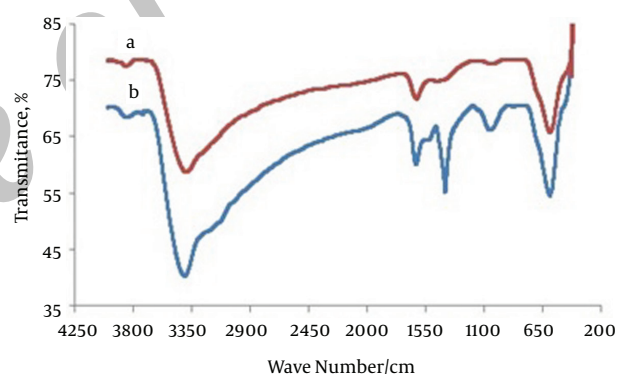| Exp. Run	Hg^{+2} conc., mg/L	pH	Adsorbent Amount	Removal, %	Predicted
1	8	6.5	0.25	95.0	94.625
2	2	6.5	0.25	90.7	91.025
3	5	5.0	0.25	96.8	97.200
4	2	5.0	0.50	97.4	96.675
5	5	6.5	0.50	97.8	97.800
6	8	5.0	0.50	98.9	98.875
7	5	8.0	0.25	95.1	94.750
8	2	8.0	0.50	88.7	88.725
9	5	8.0	0.75	95.6	95.200
10	2	6.5	0.75	89.6	89.975
11	8	6.5	0.75	99.5	99.175
12	8	8.0	0.50	98.6	99.325
13	5	6.5	0.50	97.8	97.800
14	5	5.0	0.75	99.9	100.250
15	5	6.5	0.50	97.8	97.800

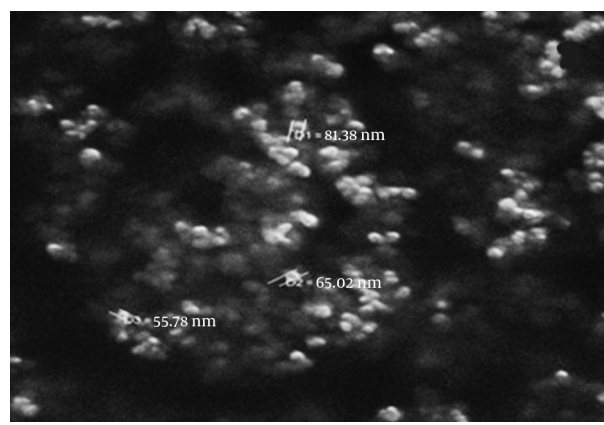**Figure 1.** FT-IR Spectra of: A) Fe_3O_4 Nanoparticles, B) CCMN

Figure 2. The SEM Photograph of CCMN

and the interaction effect of pH and the amount of adsorbent (P = 0.102). The predicted R^2 of 0.9880 and adjusted R2 of 0.9670 were in reasonable agreement, indicating the significance of the model (30). The regression coefficient for the model (0.9882) showed the goodness of fit of the model and that only 1.2% of the variation could not be explained by the regression model. Moreover, the high value of predicted regression coefficient (0.9880) showed a good correlation between experimental results and predicted responses. Using multiple regression analysis, an empirical association was observed between the percentage of mercury ions removed as the response (Y) and the three experimental variables as shown in below equation:

4) $Y = 111.464 - 0.094\,C - 6.328\,pH + 30.633\,W + 0.467\,pH \times C - 1.733\,pH \times W + 1.867\,C \times W + 0.278\,pH^2 - 0.281C^2 - 25.200\,W^2$

Where C is the initial concentration and W is the amount of adsorbent. The final mathematical model of significant actual factors for Hg^{2+} removal (Y) by the CCMNs determined by Minitab software is (30):

5) $Y = 111.464 - 6.328\,pH + 30.633\,W + 0.467\,pH \times C + 1.867\,C \times W - 0.281C^2 - 25.200\,W^2$

From equation 5, it can be concluded that the first order main effects of pH and amount of adsorbent had significant effects on removal, while the same effect for the initial concentration was insignificant ($P > 0.05$). ANOVA results (Table 3) showed that first-order effects of the main factors were more significant than their quadratic and interaction effects. Moreover, of all model components, the second-order initial concentration showed the lowest effect on Hg^{2+} removal efficiency ($P = 0.889$).

4.3. Effect of Parameters on Mercury Removal

The most important factors affecting mercury ion adsorption onto CCMN were pH, initial concentration of mercury ions, and amount of adsorbent. Surface and contour plots of these parameters showed their association with Y. In these plots, the function of two factors is examined, while the third factor is held at a constant level.
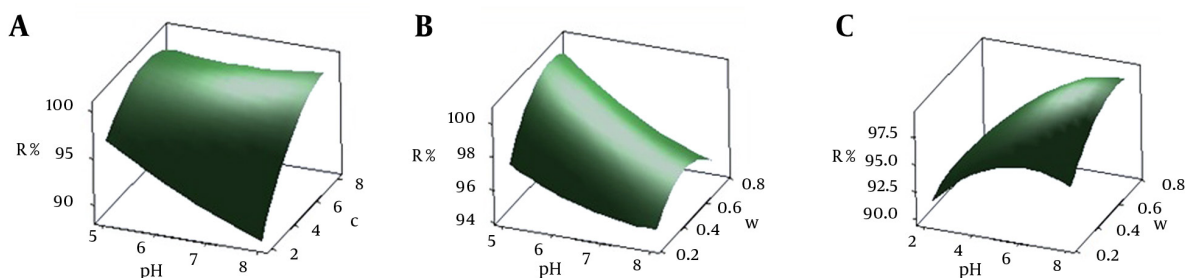
4.3.1. pH Effect

The pH values ranged from five to eight. Based on ANOVA analysis, initial pH had the greatest negative effect on adsorption. Increasing pH decreased the uptake of mercury ions. Figure 3A and 3B represent the interactive effects of pH by initial concentration of mercury ions and amount of adsorbent, respectively, on the percentage mercury ions removed as analyzed by BBD. Figure 3A shows that, as pH increased from five to eight, with metal concentration and CCMN levels kept constant, the percentage of adsorption decreased. BBD model predicted that the highest uptake of mercury should be at pH = 5 as the optimum value. This result agrees with those of the previous studies (6, 7, 27). The results of previous studies and those obtained from this study indicate that a mixture of two mechanisms might be responsible for the uptake of mercury ions by CCMN. The presence of amino groups in chitosan ($pK_a = 6.5$) helps it to adsorb transition metals via ion exchange (low pH) and complex formation mechanisms (high pH) (42). From the chitosan pK_a value, it can be assumed that, where pH = 5, amino groups on the surface of the adsorbent are protonated and adsorb mercury ions via complex formation. It has also been suggested that, for low pH in the presence of HCl, the abundance of H^+ leads to formation of anion complexes, such as $HgCl_3^-$. This anion can be adsorbed onto the CCMN via an ion exchange mechanism (7, 27). For higher pH values, the retention of Hg^{2+} decreased, probably because of the formation of metal hydroxide species (7).

4.3.2. Initial Mercury Concentration

Mercury adsorption onto CCMN was tested at initial concentrations ranging from 2 to 8 mg/L. Figure 3A and

Table 3. ANOVA for Response Surface Reduced Quadratic Model

Term	Coefficient	SE Coefficient	T	P Value
Constant	111.464	7.61163	14.644	< 0.001
pH	-6.328	2.03878	-3.104	0.027
W	30.633	8.15404	3.757	0.013
C	-0.094	0.64340	-0.147	0.889
pH × pH	0.278	0.15025	1.849	0.124
W × W	-25.200	5.40913	-4.659	0.006
C × C	-0.281	0.03756	-7.469	0.001
pH × W	-1.733	0.86615	-2.001	0.102
pH × C	0.467	0.07218	6.465	0.001
W × C	1.867	0.43308	4.310	0.008

Figure 3. Three-dimensional Response Surface Plot

A) Combined effect of pH and initial concentration; B) Combined effect of pH and adsorbent amount and; C) Combined effect of initial concentration and adsorbent amount

3C show the combined effects of initial mercury concentration with pH and amount of adsorbent. The removal percentage increased with increasing the initial mercury concentration and increased the percentage of mercury ions removed for values from to 2 to 6 mg/L and then decreased slightly for higher values. This finding is in agreement with previous studies and can be attributed to the driving force that overcomes all mass transfer resistance of metal between the aqueous and solid phases (29, 33, 43, 44). Furthermore, it can be assumed that increasing initial metal concentration increases the number of collisions between mercury ions and CCMNs, thus increasing adsorption. BBD analysis predicted that the maximum removal of mercury ions would occur for an initial mercury concentration of 6.2 mg/L.

4.3.3. Adsorbent

The results of the combined effects of the amount of adsorbent with pH and initial metal concentration are shown in Figure 3B-D response surface plots and contours. Figure 3B shows that increasing the amount of adsorbent from 0.25 g to 0.75 g while keeping the pH = 5 and initial mercury concentration constant (6.2 mg/L), increases the percentage of removal of Hg^{2+} by CCMN. The higher mass of adsorbent means that more surface area, including functional groups, is available. BBD analysis predicted the optimum amount of damp adsorbent to be 0.67 g, which is equivalent to 67 mg of dried CCMN. Finally the optimum values for independent variables of pH, mercury and amount of adsorbent were 5, 6.2 mg/L and 67 mg, respectively.

4.4. Kinetic Studies

The effect of contact time on the adsorption of mercury ions under optimal conditions (pH = 5, initial metal concentration = 6.2 mg/L and amount of damp adsorbent = 0.67 g) was studied. The results showed that the adsorption rate was high and reached equilibrium in < 5 minutes with 99.91% of the mercury ions adsorbed. This rapid adsorption might be due to chemical binding or electrostatic attraction between mercury ions and surface functional groups (4). Three kinetic models (pseudo first-order, pseudo second-order, and intra-particle diffusion) were used to test the experimental data and verify the kinetic mechanism of sorption. The linear form of the pseudo second-order equation is:

6) $t/q_t = 1/k_2 q_e^2 + t/q_e$

Where k_2 (g/mg/min) is the pseudo second-order rate constant of adsorption. A plot of t/q_t versus t (Figure 4) yielded a very good straight line and correlation coefficient. In addition, q_e (4.44 mg/g) agreed well with the calculated q_e (4.48 mg/g) value revealing that adsorption of Hg^{2+} onto the CCMN follows a pseudo second-order mechanism. This trend suggests that a chemisorption reaction via the amino groups on the surface of the CCMN, a high specific surface area, and the absence of internal

diffusion predominate in the rate controlling step. It is likely that sharing of electrons between anions and the adsorbent produced valence forces in the adsorption process (26, 27). These results are consistent with other investigations (37).

4.5. Adsorption Isotherms

It is important to investigate equilibrium adsorption isotherms in the design of adsorption system and to explain the interactive behavior of the metal ions and solid phase. To generate equilibrium adsorption data in this study, the Langmuir and Freundlich isotherm models were employed. To study these adsorption isotherms, initial mercury ion concentrations were set in the range of 1-15 mg/L under optimal conditions (pH = 5, and amount of wet adsorbent = 0.67 g). The Langmuir isotherm model is expressed as:

7) $C_e/q_e = C_e/q_m + 1/K_L q_m$

Where C_e (mg/L) is the equilibrium concentration of the metal ions, q_e (mg/g) is the percentage of metal ions adsorbed under equilibrium conditions, q_m (mg/g) is the maximum adsorption capacity, and K_L (L/mg) is the Langmuir constant (a measure of the affinity of binding sites and is a measure of the adsorption energy). The Langmuir isotherm assumes that uptake occurs on a homogeneous surface by monolayer adsorption without interaction between the absorbed materials. Plotting C_e/q_e against C_e gives a straight line and q_m and K_L can be calculated from the slope and intercept of the plot, respectively. Another important parameter, the separation factor (R_L), shows a degree of suitability of the adsorbent toward the metal ions and is calculated using binding constant K_L as:

8) $R_L = 1/(1 + C_i K_L)$

Where C_i is the initial concentration of the metal ion. The adsorption process can be defined by the magnitude of R_L as: $R_L > 1.0$ is unsuitable; $R_L = 1$ is linear; $0 < R_L < 1$ is suitable; $R_L = 0$ is irreversible (27). The Freundlich isotherm differs from the Langmuir isotherm model. It describes multilayer adsorption and adsorption on heterogeneous surfaces. The experimental data was fitted to the linear Freundlich equation as:
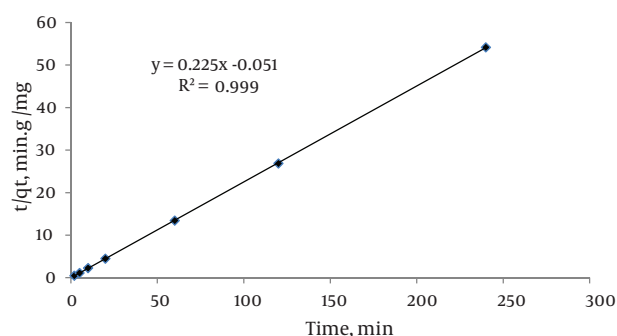

Figure 4. Pseudo Second Order Kinetic Plot for the Adsorption of Hg^{2+} on CCMN (Initial Concentration 6.2 mg/L, CCMN Amount 67 mg and pH = 5)

9) $\log q_e = \log K_F + 1/n \log C_e$

Where K_F (mg/g) and $1/n$ (L/mg) are the Freundlich constants for adsorption capacity and energy of adsorption, respectively. Table 4 presents the parameters obtained by implementing the Langmuir and Freundlich models using the experimental data. As shown in Table 4, correlation coefficient R^2 for the Langmuir isotherm is 0.949, which indicates that the adsorption of mercury onto the CCMN is favorable. The R_L calculated for 1-15 mg/L concentrations of mercury ions at pH = 5 and damped adsorbent = 0.67 g lie between 0.01 and 0.13, indicating that Hg^{2+} adsorption onto CCMN was linear.

Table 4 shows that the plot of the Freundlich isotherm had an acceptable fit with a correlation coefficient of 0.943, suggesting the presence of heterogamous conditions. The small value of $1/n$ (0.407), between 0 and 1, and the large value of KF (7.01 mg/g) show that mercury ions can be effectively adsorbed by CCMN (4, 45, 46). It can be concluded that both isotherm models are adequate to describe the adsorption process mechanism for the studied concentration range.

5. Discussion

In this study, the Box-Behnken methodology was used to find the feasibility and the adsorbent for the removal of mercury ion from aqueous solutions. This approach proved to be an effective and time saving method to study the influence of major process factors (pH, concentration, amount of adsorbent) and determine optimal conditions for the removal of mercury ions while significantly reducing the required number of experiments. This model indicated that 99.91% removal of Hg^{2+} is possible at optimal conditions of pH = 5, mercury ion concentration = 6.2 mg/L, and amount of damped adsorbent = 0.67 g (equivalent to 67 mg of dried CCMN). The results showed that CCMN is an excellent adsorbent for low and moderate concentrations of mercury ions, which is the usual amount found in water and waste aqueous solutions.

The adsorption isotherm was well fitted by both the Langmuir and Freundlich models. Kinetic studies of the adsorption process confirmed the efficiency of the pseudo second-order kinetic model. The high initial adsorption rate and short equilibrium uptake time indicated that the surface of CCMN has a high density of active sites

for mercury ion uptake. This proposed method applies an environmentally friendly non-toxic adsorbent which does not threaten human health. In addition, the critical step of separation of the treated solution from the adsorbent can be accomplished easily using an external magnetic field.

Authors' Contribution

Dr. Jahangiri and Dr. Khodayar: developed the original idea; Dr. Rahbar: study concept and design of experiments, acquisition of data, analysis and interpretation of data, writing of the manuscript; Mr. Boumi: conducted the experimental section.

Financial Disclosure

There is no conflict of interest.

References

1. Pan S, Shen H, Xu Q, Luo J, Hu M. Surface mercapto engineered magnetic Fe3O4 nanoadsorbent for the removal of mercury from aqueous solutions. *J Colloid Interface Sci.* 2012;**365**(1):204–12.
2. Girginova PI, Daniel-da-Silva AL, Lopes CB, Figueira P, Otero M, Amaral VS, et al. Silica coated magnetite particles for magnetic removal of Hg2+ from water. *J Colloid Interface Sci.* 2010;**345**(2):234–40.
3. Parham H, Zargar B, Shiralipour R. Fast and efficient removal of mercury from water samples using magnetic iron oxide nanoparticles modified with 2-mercaptobenzothiazole. *J Hazard Mater.* 2012;**205-206**:94–100.
4. Hakami O, Zhang Y, Banks CJ. Thiol-functionalised mesoporous silica-coated magnetite nanoparticles for high efficiency removal and recovery of Hg from water. *Water Res.* 2012;**46**(12):3913–22.
5. Goyal M, Bhagat M, Dhawan R. Removal of mercury from water by fixed bed activated carbon columns. *J Hazard Mater.* 2009;**171**(1-3):1009–15.
6. Ma F, Qu R, Sun C, Wang C, Ji C, Zhang Y, et al. Adsorption behaviors of Hg(II) on chitosan functionalized by amino-terminated hyperbranched polyamidoamine polymers. *J Hazard Mater.* 2009;**172**(2-3):792–801.
7. Zhou L, Liu Z, Liu J, Huang Q. Adsorption of Hg(II) from aqueous solution by ethylenediamine-modified magnetic crosslinking chitosan microspheres. *Desalination.* 2010;**258**(1–3):41–7.
8. Qu R, Sun C, Ma F, Zhang Y, Ji C, Xu Q, et al. Removal and recovery of Hg(II) from aqueous solution using chitosan-coated cotton fibers. *J Hazard Mater.* 2009;**167**(1-3):717–27.
9. Takagai Y, Shibata A, Kiyokawa S, Takase T. Synthesis and evaluation of different thio-modified cellulose resins for the removal of mercury (II) ion from highly acidic aqueous solutions. *J Colloid Interface Sci.* 2011;**353**(2):593–7.
10. Chang MY, Juang RS. Adsorption of tannic acid, humic acid, and dyes from water using the composite of chitosan and activated clay. *J Colloid Interface Sci.* 2004;**278**(1):18–25.
11. Tiwari DK, Behari J, Sen P. Application of Nanoparticles in Waste

Table 4. The Langmuir and Freundlich Parameters for Adsorption of Hg^{2+} Onto CCMN

	Langmuir	Freundlich
q_{max}, mg/g	9.34	-
K, L/mg	6.69	7.01
R^2	0.949	0.934
R	0.01-0.13	-
1/n	-	0.41

Water Treatment 1. *World Appli Sci.* 2008;**3**:417–33.

12. Qu X, Alvarez PJ, Li Q. Applications of nanotechnology in water and wastewater treatment. *Water Res.* 2013;**47**(12):3931–46.

13. Brar SK, Verma M, Tyagi RD, Surampalli RY. Engineered nanoparticles in wastewater and wastewater sludge--evidence and impacts. *Waste Manag.* 2010;**30**(3):504–20.

14. Zargar B, Parham H, Hatamie A. Modified iron oxide nanoparticles as solid phase extractor for spectrophotometeric determination and separation of basic fuchsin. *Talanta.* 2009;**77**(4):1328–31.

15. Parham H, Rahbar N. Solid phase extraction-spectrometric determination of fluoride in water samples using magnetic iron oxide nanoparticles. *Talanta.* 2009;**80**(2):664–9.

16. Wan Ngah WS, Teong LC, Hanafiah MAKM. Adsorption of dyes and heavy metal ions by chitosan composites: A review. *Carbohydr Polym.* 2011;**83**(4):1446–56.

17. Guibal E. Interactions of metal ions with chitosan-based sorbents: a review. *Sep Pur Tech.* 2004;**38**(1):43–74.

18. Ravi Kumar MNV. A review of chitin and chitosan applications. *React Funct Polym.* 2000;**46**(1):1–27.

19. Domard A. A perspective on 30 years research on chitin and chitosan. *Carbohydr Polym.* 2011;**84**(2):696–703.

20. Minagawa T, Okamura Y, Shigemasa Y, Minami S, Okamoto Y. Effects of molecular weight and deacetylation degree of chitin/chitosan on wound healing. *Carbohydr Polym.* 2007;**67**(4):640–4.

21. Vasnev VA, Tarasov AI, Markova GD, Vinogradova SV, Garkusha OG. Synthesis and properties of acylated chitin and chitosan derivatives. *Carbohydr Polym.* 2006;**64**(2):184–9.

22. Jayakumar R, Nwe N, Tokura S, Tamura H. Sulfated chitin and chitosan as novel biomaterials. *Int J Biol Macromol.* 2007;**40**(3):175–81.

23. Rinaudo M. Chitin and chitosan: Properties and applications. *Prog Polym Sci.* 2006;**31**(7):603–32.

24. Elwakeel KZ. Removal of Cr(VI) from alkaline aqueous solutions using chemically modified magnetic chitosan resins. 2010;**250**(1):105–12.

25. Fan L, Li M, Lv Z, Sun M, Luo C, Lu F, et al. Fabrication of magnetic chitosan nanoparticles grafted with beta-cyclodextrin as effective adsorbents toward hydroquinol. *Colloids Surf B Biointerfaces.* 2012;**95**:42–9.

26. Fan L, Luo C, Lv Z, Lu F, Qiu H. Preparation of magnetic modified chitosan and adsorption of Zn(2)(+) from aqueous solutions. *Colloids Surf B Biointerfaces.* 2011;**88**(2):574–81.

27. Monier M, Abdel-Latif DA. Preparation of cross-linked magnetic chitosan-phenylthiourea resin for adsorption of Hg(II), Cd(II) and Zn(II) ions from aqueous solutions. *J Hazard Mater.* 2012;**209-210**:240–9.

28. Paulino AT, Belfiore LA, Kubota LT, Muniz EC, Almeida VC, Tambourgi EB. Effect of magnetite on the adsorption behavior of Pb(II), Cd(II), and Cu(II) in chitosan-based hydrogels. *Desalination.* 2011;**275**(1–3):187–96.

29. Peng Q, Liu Y, Zeng G, Xu W, Yang C, Zhang J. Biosorption of copper(II) by immobilizing Saccharomyces cerevisiae on the surface of chitosan-coated magnetic nanoparticles from aqueous solution. *J Hazard Mater.* 2010;**177**(1-3):676–82.

30. Islam MA, Sakkas V, Albanis TA. Application of statistical design of experiment with desirability function for the removal of or-
ganophosphorus pesticide from aqueous solution by low-cost material. *J Hazard Mater.* 2009;**170**(1):230–8.

31. Yetilmezsoy K, Demirel S, Vanderbei RJ. Response surface modeling of Pb(II) removal from aqueous solution by Pistacia vera L.: Box-Behnken experimental design. *J Hazard Mater.* 2009;**171**(1-3):551–62.

32. Ozdemir E, Duranoglu D, Beker U, Avcı AO. Process optimization for Cr(VI) adsorption onto activated carbons by experimental design. *Chem Engin J.* 2011;**172**(1):207–18.

33. Mourabet M, El Rhilassi A, El Boujaady H, Bennani-Ziatni M, El Hamri R, Taitai A. Removal of fluoride from aqueous solution by adsorption on Apatitic tricalcium phosphate using Box–Behnken design and desirability function. *Appl Surf Sci.* 2012;**258**(10):4402–10.

34. Geyikci F, Kılıc E, Coruh S, Elevli S. Modelling of lead adsorption from industrial sludge leachate on red mud by using RSM and ANN. *Chem Engin J.* 2012;**183**:53–9.

35. Ebrahimzadeh H, Behbahani M, Yamini Y, Adlnasab L, Asgharinezhad AA. Optimization of Cu(II)-ion imprinted nanoparticles for trace monitoring of copper in water and fish samples using a Box–Behnken design. *React Funct Polym.* 2013;**73**(1):23–9.

36. Khajeh M. Application of Box-Behnken design in the optimization of a magnetic nanoparticle procedure for zinc determination in analytical samples by inductively coupled plasma optical emission spectrometry. *J Hazard Mater.* 2009;**172**(1):385–9.

37. Namdeo M, Bajpai SK. Chitosan–magnetite nanocomposites (CMNs) as magnetic carrier particles for removal of Fe(III) from aqueous solutions. *Colloids Surf A Physicochem Eng Asp.* 2008;**320**(1–3):161–8.

38. Parham H, Rahbar N. Solid phase extraction-spectrophotometric determination of salicylic acid using magnetic iron oxide nanoparticles as extractor. *J Pharm Biomed Anal.* 2009;**50**(1):58–63.

39. Khan H, Ahmed MJ, Bhanger MI. A simple spectrophotometric determination of trace level mercury using 1,5-diphenylthiocarbazone solubilized in micelle. *Anal Sci.* 2005;**21**(5):507–12.

40. Franson MAH. American public health association American water works association water environment federation. *Methods.* 1995;**6**:84.

41. Kousha M, Daneshvar E, Dopeikar H, Taghavi D, Bhatnagar A. Box–Behnken design optimization of Acid Black 1 dye biosorption by different brown macroalgae. *Chem Engin J.* 2012;**179**:158–68.

42. Miretzky P, Cirelli AF. Hg(II) removal from water by chitosan and chitosan derivatives: a review. *J Hazard Mater.* 2009;**167**(1-3):10–23.

43. Aksu Z, Tezer S. Biosorption of reactive dyes on the green alga Chlorella vulgaris. *Process Biochem.* 2005;**40**(3–4):1347–61.

44. Malkoc E, Nuhoglu Y. Potential of tea factory waste for chromium(VI) removal from aqueous solutions: Thermodynamic and kinetic studies. *Sep Pur Tech.* 2007;**54**(3):291–8.

45. Zhang FS, Itoh H. Adsorbents made from waste ashes and postconsumer PET and their potential utilization in wastewater treatment. *J Hazard Mater.* 2003;**101**(3):323–37.

46. Pan S, Zhang Y, Shen H, Hu M. An intensive study on the magnetic effect of mercapto-functionalized nano-magnetic Fe3O4 polymers and their adsorption mechanism for the removal of Hg(II) from aqueous solution. *Chem Engin J.* 2012;**210**:564–74.